

# THE TRANSFORMATION FROM TIME TO FREQUENCY DOMAIN

**AUTHORS' NOTE**

Pieter Nuij, senior system architect, and David Rijlaarsdam, group leader, both work at NTS Systems Development in Eindhoven, the Netherlands.

[pieter.nuij@nts-group.nl](mailto:pieter.nuij@nts-group.nl)  
[www.nts-group.nl](http://www.nts-group.nl)

A series of three articles will feature Frequency Response Function (FRF) measurements. The FRF, describing the frequency-dependent behaviour of linear systems, is an indispensable tool in the engineering of dynamic systems. This series is not meant to be mathematically rigorous but aims at an understanding of the main steps to determine the FRF based on real measurements from an application point of view. Part 1 deals with the transformation of time-domain signals to the frequency domain and may serve as a stand-alone guide for basic signal analysis.

PIETER NUIJ AND DAVID RIJLAARDAM

**Why transform?**

Although we 'live' in the time domain and naturally ask ourselves *when* things happen, asking the question *how often* things happen often leads to revealing answers. Figure 1 shows a time signal of the torque measured through the outgoing shaft of a gearbox. The spectrum of the same signal is displayed in Figure 2 and clearly shows discrete frequency components that can be related to the gear ratios of the gearbox. Although the time signal also contains this information, it is not visible in the time trace in Figure 1.

**Discrete spectrum**

To determine the spectrum of a continuous time signal the signal must be converted into a sequence of numbers that form the input for a numerical algorithm running in a computer. Figure 3 shows the necessary steps for this conversion.

The continuous time signal is conditioned and amplified/attenuated in an analogue electronics stage before it is low-pass-filtered to limit its frequency content. After filtering, the signal is sampled and becomes a discrete time signal. The individual samples are converted from an analogue signal into a quantised signal with discrete values.

Limiting the frequency content of the continuous time signal before sampling is important, but it is sometimes neglected, causing erroneous results. Figure 4a shows a continuous time signal with frequency  $f_{\text{signal}}$  that is sampled with sampling frequency  $f_{\text{sample}}$ . The resulting discrete time signal is a true representation of the continuous time signal. In Figure 4b a different signal with frequency  $f_{\text{signal}} + f_{\text{sample}}$  is sampled with the same sampling frequency  $f_{\text{sample}}$ . The reconstructed discrete time signal seems to be the representation of a continuous time signal with frequency  $f_{\text{signal}}$ .

This example clearly shows that sampling can introduce errors called aliasing components. To prevent this from

## Three articles

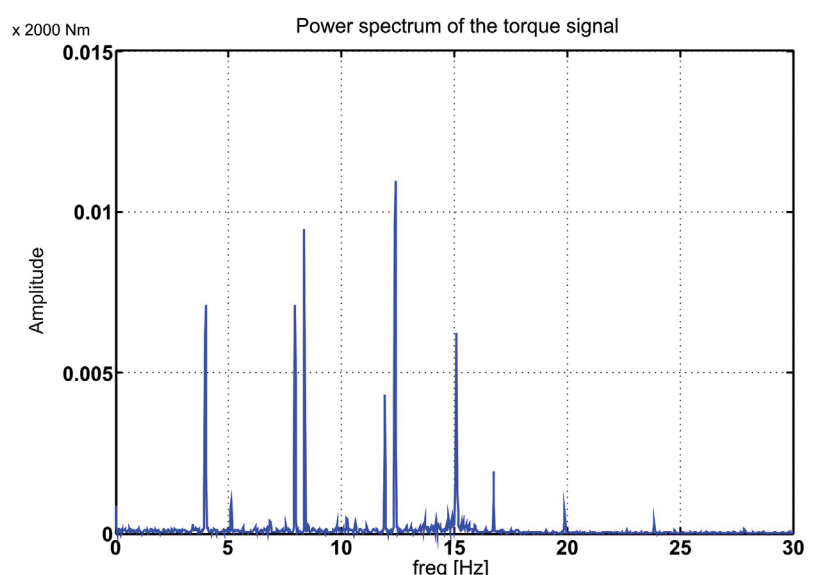
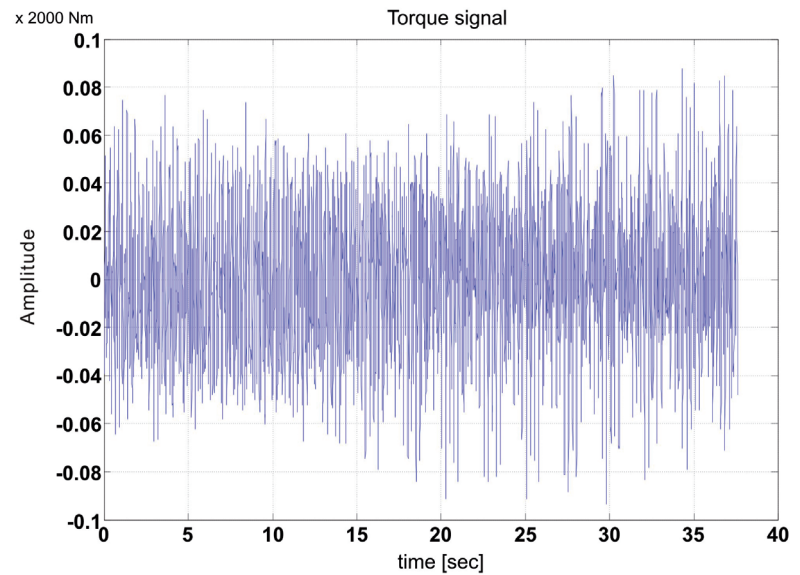
This article covers the steps that are necessary to convert a time-continuous signal into a discrete spectrum. Potential errors due to aliasing and leakage will be explained and solutions will be presented. An overview of several types of test signals will be presented. The second article will introduce the FRF, explaining the choice of test signals in their relation to the coherence function and the measurement of the FRF in open-loop and in closed-loop systems. The third article will focus on the extension of frequency-domain methods towards nonlinear systems and the application of such methods to define and optimise the performance of such systems. Each article will be illustrated with examples.



- 1 Time trace of torque measurement.
- 2 Spectrum of torque measurement.
- 3 Necessary steps to convert a continuous time signal into numerical data points.

happening, the sampling frequency must be at least twice the frequency of the highest frequency component present in the continuous time signal. Since the frequency content of the signal to be analysed is often unknown, low-pass filtering to limit the frequency content is required. The filter used for this purpose is called an anti-aliasing filter.

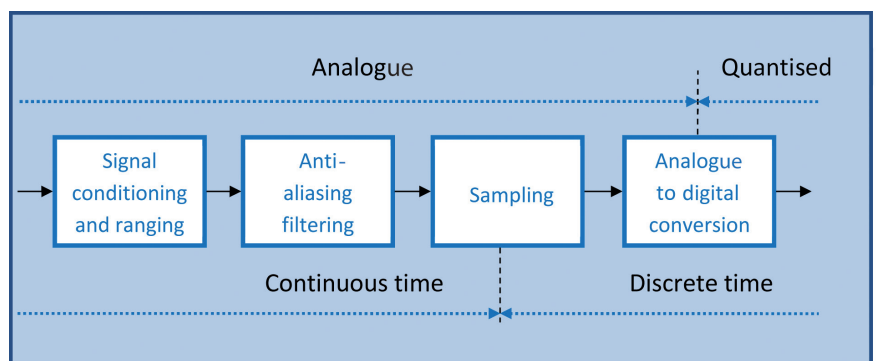
Like any filter the anti-aliasing filter will introduce frequency-dependent phase shifts in the filtered signal. This is not a problem when measuring FRFs as long as all measurement channels used for the FRF calculations experience equal phase shift. In the last block in Figure 3 the discrete time analogue signal is quantised, rounded to the nearest discrete amplitude value of the  $2^n$  possible values that can be represented by an  $n$ -bits digital word. Optimal use of the amount of bits requires matching of the amplitude of the signal to the voltage range that can be accommodated by the AD converter (ADC). This is done by choosing the correct amplification or attenuation factors in the signal-conditioning front-end. Poor ranging will cause harmonic distortion and a high noise floor but due to the advent of high-quality 24-bits ADCs the ranging requirements become less stringent.

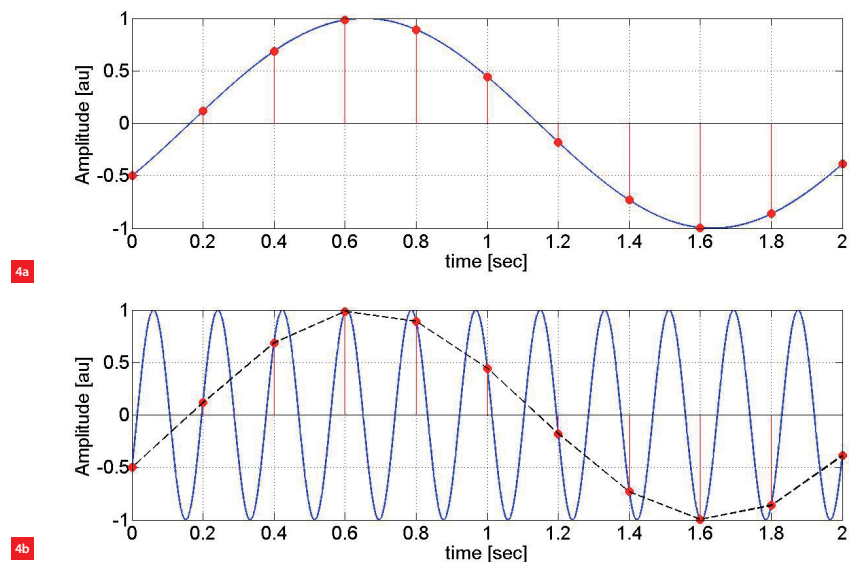


## Certified Precision Engineer competencies

The content of this series of three articles is in part covered in the "Experimental Techniques in Mechatronics" course, provided by The High Tech Institute (HTI). This course has been selected for the DSPE Certification Program (see page 58).

[WWW.DSPEREGISTRATION.NL](http://WWW.DSPEREGISTRATION.NL) | [WWW.HIGHTECHINSTITUTE.NL](http://WWW.HIGHTECHINSTITUTE.NL)



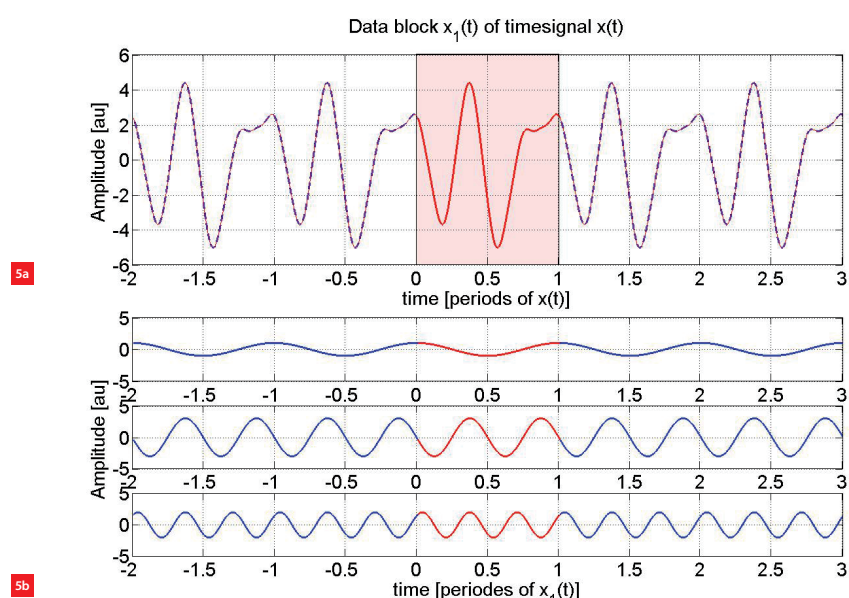


### 4 Introduction of errors by sampling.

- (a) Signal (blue) with frequency  $f_{\text{signal}}$  sampled with frequency  $f_{\text{sample}}$  (red).
- (b) Signal (blue) with frequency  $f_{\text{signal}} + f_{\text{sample}}$  sampled with frequency  $f_{\text{sample}}$  (red). The reconstructed signal is the aliasing component (black).

### 5 Analysis of time signal $x(t)$ in blue.

- (a) Periodically reconstructed time signal based on measurement signal  $x_1(t)$  in red.
- (b) Some of the signal components present in  $x_1(t)$ .



### Frequency analysis

The common way to describe the frequency content of a time signal is to use a series of cosines with specific frequencies, amplitudes and phases. The Fast Fourier Transform (FFT) is a very efficient algorithm for calculating these cosine-based signal components. However, as will be demonstrated, the results must be interpreted carefully.

Figure 5a shows a time signal  $x(t)$  of which frequency components are to be identified (= transformed from time to frequency domain). Since the signal is periodic with a period of  $T$ , it consists of a series of cosine components

with frequencies being a multiple of  $1/T \text{ Hz}$ . So if  $T$  is 1 s,  $x(t)$  will consist of a series of harmonics of 1 Hz.

A segment  $x_1(t)$  of  $x(t)$  is captured and this measurement record will be processed. If the length  $T_1$  of the segment  $x_1(t)$  is equal to  $T$ , then the result of the FFT will correctly describe the frequency content of the time signal  $x(t)$ . This can be seen in Figure 5a, where the repetition of the measurement record  $x_1(t)$  results in a signal equal to the original signal  $x(t)$ . Figure 5b shows some of the cosine components present in the signal. The amplitude and phase values of these cosine components are plotted in the amplitude and phase spectra as displayed in Figure 6. The units on the x axis in Figure 6 are cycles/ $T_1$ , with  $T_1$  the period time of the measurement record  $x_1(t)$ .

$T_1$  can be calculated from the sampling frequency ( $f_s$ ) and the size of the measurement record:

$$T_1 = \# \text{ samples} / f_s$$

Knowing  $T_1$ , the frequency axis can be scaled to cycles per second [Hz]. The resulting frequency resolution  $\Delta f$  of the spectrum is equal to  $1/T_1$ . The highest frequency component that can be present in the spectrum has a value of  $f_s/2 \text{ Hz}$ . If a different segment of  $x(t)$  is captured, but the length of the segment remains  $T_1$ , the amplitude spectrum will remain the same but the phase spectrum will be different. If the length of the segment is changed, the amplitude spectrum will also change.

Figure 7 shows the situation that  $T_2$ , the length of the measurement record  $x_2(t)$ , is not an integer amount of periods  $T$  of  $x(t)$  any longer. The FFT algorithm will again determine the best fit of a series of cosines, but this time

**6** Spectra of measurement signal  $x_1(t)$  in case the measurement record length  $T_1$  is equal to period  $T$ .  
 (a) Amplitude.  
 (b) Phase.

**7** Results in case the measurement record length  $T_2$  is not an integer amount of periods  $T$ .  
 (a) Time signal  $x(t)$  in blue and periodically reconstructed time signal based on measurement signal  $x_1(t)$  in red.  
 (b) Amplitude and phase spectra of measurement signal  $x_1(t)$  in blue and  $x_2(t)$  in red, both with starting time  $t = 0$  s.

their frequencies will be multiples of  $1/T$ . This series, however, describes a time signal with period  $T_2$ , shown as the red curve in Figure 7a. This signal clearly differs from the original signal  $x(t)$ , which has a period time  $T$  of 1 s. The calculated amplitude and phase spectra in Figure 7b in red will differ from the true spectra in blue. This measurement error is called ‘leakage’ and will always be present unless the length of the measurement record is an exact multiple of the period  $T$  of the signal to be analysed. In the frequency analysis of stochastic signals (noise) this error will always occur, since these signals are non-periodic. The leakage error, however, can be reduced by the application of weighting functions.

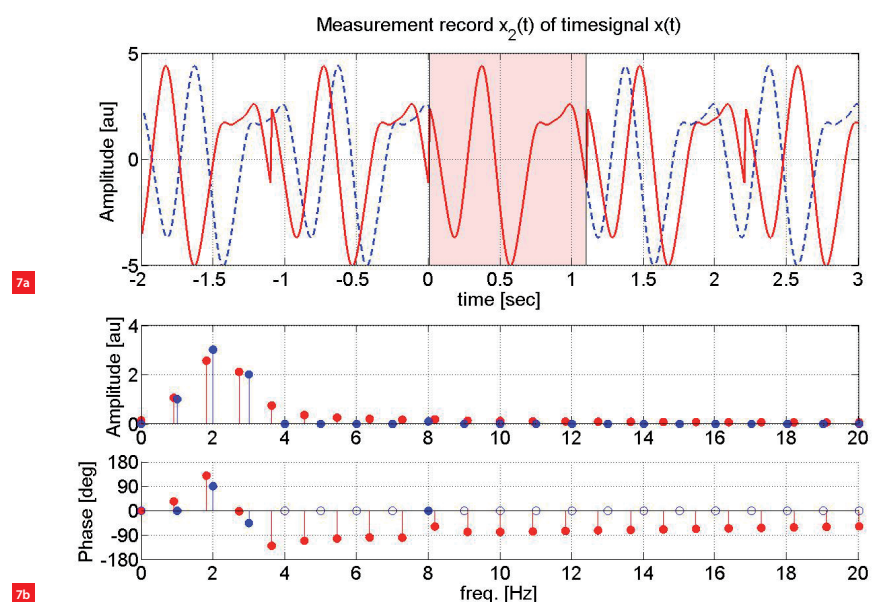
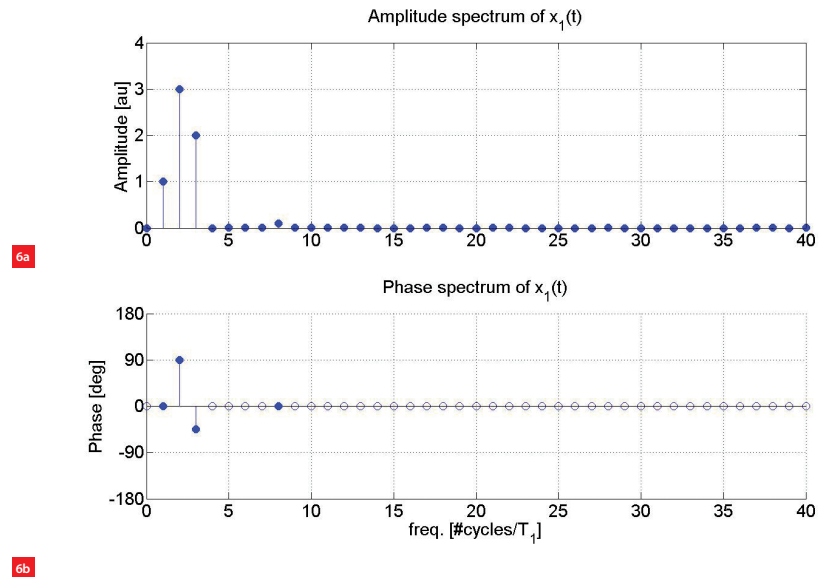
The Hanning weighting function is a commonly used general purpose weighting function and is defined as:

$$w(t) = \sqrt{(8/3)} \cdot \sin^2(2\pi t/T)$$

Here,  $T$  is the record length.

In Figure 8a the weighting function is depicted in black. Applying this weighting function to  $x_2(t)$  results in a new time trace  $x_{2\text{hanning}}(t) = w(t) \cdot x_2(t)$ , which represents a signal with reduced discontinuities, see Figure 8a in red. Figure 8b shows the spectra of  $x_1(t)$  in blue,  $x_2(t)$  in red and  $x_{2\text{hanning}}(t)$  in black in a logarithmic amplitude format. The leakage error in  $x_2(t)$  is clearly visible. This error even obscures the presence of a weak signal component at 8 Hz.

Applying a Hanning weighting function significantly reduces the leakage error, but it cannot be applied to all signals. Since  $w(t)$  is not a constant but a function of time, this type of weighting is only allowed for signals with time-



independent characteristics. This does not require the signal to be periodic. A noise signal with time-independent mean and variance also fulfils this criterion.

In modal analysis a transient signal (hammer impact) is often used for system excitation. A transient weighting function is applied to improve the signal-to-noise ratio for the analysis of these short transient signals. The transient weighting function is defined as:

$$w(t) = 1 \quad \text{for } t_0 \leq t < t_0 + t_w \text{ and } 0 \leq t_0 < T - t_w$$

$$w(t) = 0 \quad \text{elsewhere}$$

## INTRODUCTION TO FREQUENCY RESPONSE FUNCTION MEASUREMENTS – PART 1

Here,  $t_0$  is the moment the window opens and  $t_w$  the length of the window. The system response signal is also a transient and prone to leakage if the system has low damping and must be weighted with an exponential decay window. This window is defined as:

$$w(t) = e^{-(t-t_0)/\tau} \text{ for } t_0 \leq t < T \text{ and } 0 \leq \tau < T$$

$$w(t) = 0 \quad \text{elsewhere}$$

8a

Here,  $t_0$  is the starting time of the weighting function,  $\tau$  the time constant and  $T$  the record length. Figure 9a shows the transient window and Figure 9b the exponential decay window, both dashed in black.

### Signal units

So far the focus was on periodic signals that consist of a series of discrete frequency components with constant amplitudes. Their power distribution over frequency is discrete, so the power is concentrated in infinitesimally narrow frequency lines. The ‘strength’ of these components is independent of the frequency resolution of the spectrum and can be calculated from the FFT lines like:

$$\text{Ampl}(k \cdot \Delta f) = |f(k)| \quad \text{with amplitude in [units]}$$

or

$$\text{Ampl}(k \cdot \Delta f) = |f(k)| / \sqrt{2} \quad \text{with amplitude in [units RMS]}$$

8b

Here,  $f(k)$  is the  $k^{\text{th}}$  frequency line at  $(k - 1) \cdot \Delta f$  [Hz].

Signals with a continuous power distribution cannot be quantified with amplitude values. These signals are to be quantified by their Power Spectral Density as function of frequency,  $PSD(f)$ .

$PSD(f)$  can be calculated from the individual FFT lines by averaging the power per line and scaling it with the equivalent noise bandwidth  $ENB$  of the FFT calculation:

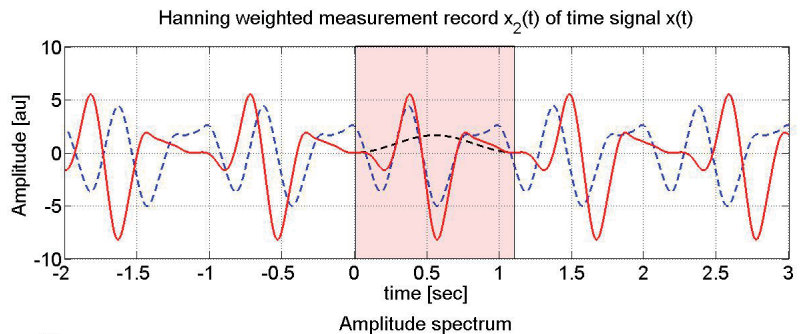
$$PSD(k \cdot \Delta f) = \overline{|f(k)|^2} / ENB \quad [\text{units}^2/\text{Hz}]$$

The  $ENB$  depends on the record length and the weighting function used:

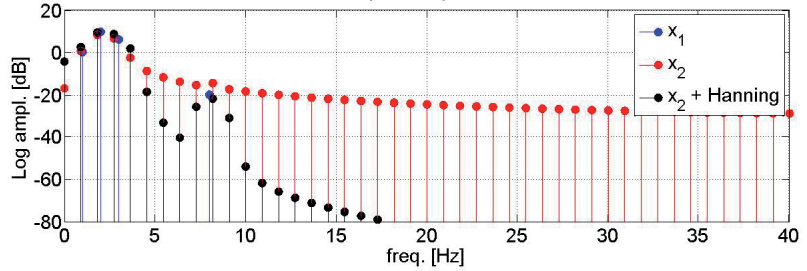
$$ENB = \Delta f \cdot \text{window\_factor}$$

For a rectangular weighting function (= no weighting function)  $\text{window\_factor} = 1$ , for Hanning  $\text{window\_factor} = 1.5$ .

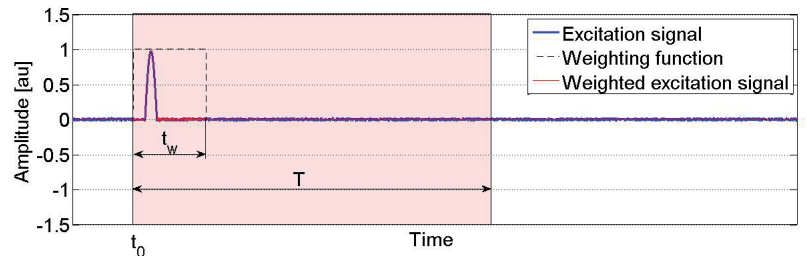
For signals with a finite total energy, like transients, the Energy Spectral Density as function of frequency  $ESD(f)$  can be calculated from the individual FFT lines by



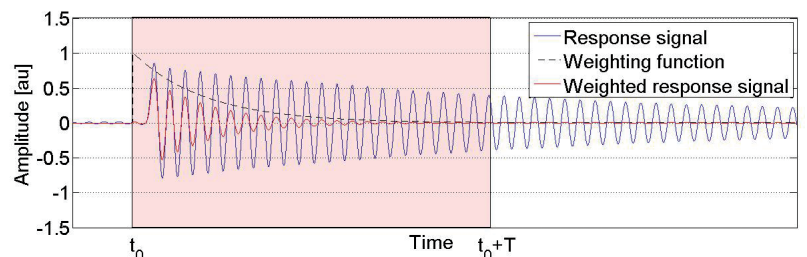
8a



8b



9a



9b

8 The aim of the Hanning weighting function.

(a) The function (in black) smoothens out the discontinuities at the beginning and end of the measurement record and thus reduces leakage.  
 (b) Leakage can obscure signal components.

9 To be used for transient signals:

(a) transient weighting function;  
 (b) exponential decay function.

averaging the power per line and scaling it with the equivalent noise bandwidth of the FFT calculation and the record length:

$$ESD(k \cdot \Delta f) = \overline{|f(k)|^2} \cdot T / ENB \quad [\text{units}^2 \text{ s/Hz}]$$

### Test signals

Test signals play a decisive role in measuring the FRF of a dynamic system. Important parameters are frequency content, power and amplitude distribution as function of time and the relation between peak value and RMS value (= crest factor).

The most basic test signal is the sinusoid. If the frequency is a multiple of the frequency resolution  $\Delta f = 1/T$ , then no weighting function is required. The crest factor is only  $\sqrt{2}$ , which makes it a well-suited signal for testing extremely delicate systems. The sinusoid is ideal for measuring the Higher Order Sinusoidal Input Describing Functions (HOSIDF) to determine nonlinear behaviour, as will be discussed in Part 3 of this series. Since all power is contained in only one frequency line, many measurements are required to cover a frequency range.

Measurement time can be reduced by constructing a test signal that contains power at many frequency lines at the same time. These multi-sine signals can be processed without weighting function if all the frequency components coincide with frequency lines of the FFT. The crest factor can be minimised by manipulating the phase of all frequency components and can even become less than  $\sqrt{2}$ .

In a special class of multi-sine signals distinct frequency lines do not contain energy. If a nonlinear system is excited by these special odd multi-sines, its response will contain power in the non-excited frequency lines, which serve as detection lines for nonlinear behaviour. It is important to realise that these signals are periodic and thus consist of frequency components with a fixed amplitude and phase. In Part 2 it will become clear that for this reason multi-sines

cannot be used for coherence measurements when only one phase realisation is used.

Unlike multi-sine signals, random noise has a continuous spectrum and is not periodic. This results in leakage and so the use of a Hanning weighting function is required. The frequency range can be optimised by filtering. Within this range the PSD can be flat (white noise) or inversely proportional with frequency (pink noise). Noise is uncorrelated with all other signals. The cross-spectrum of noise and any other signal will converge to 0 after averaging, as will be explained in Part 2. This property is used to determine the frequency response function of a system under non-ideal measurement conditions.

The pulse signal differs from the test signals mentioned earlier in the sense that its power distribution over frequency is time-dependent. For modal analysis measurements the pulse is generated by a hammer impact. By changing the hardness of the hammer tip, the frequency range of the pulse spectrum can be influenced. A soft tip will result in a wider pulse, which contains less high-frequency energy. As mentioned in the paragraph on weighting functions, an impact window can be used to increase the signal-to-noise ratio of the measurement. Triggering is important to align the window with the pulse. To capture the total pulse, a pre-trigger delay is required. ■

## Summary

Signal	Units	Weighting function	Trigger condition
Sine $f = n \cdot \Delta f$	Ampl. [units]	None Hanning	Free run
Sine $f \neq n \cdot \Delta f$	Ampl. [units]	None	Free run
Multi-sine, linked to $\Delta f$	PSD [units <sup>2</sup> /Hz]	Hanning	Free run
Random	ESD [units <sup>2</sup> s/Hz]	Transient window	Pre-triggered on pulse
Pulse			

## Coming up in Part 2

In Part 2 the Frequency Response Function will be introduced as the frequency-domain description of dynamic behaviour of linear dynamic systems. The article will focus on the practical aspects of FRF measurements: choice of test signals, picket-fence effect, measurement noise, and interpretation of the coherence function for detection of nonlinearities. Both open-loop and closed-loop systems will be considered.

## LITERATURE

- J.S. Bendat, A.G. Piersol, "Random data: analysis and measurement procedures", Chichester: Wiley-Interscience, 2000, ISBN 0-471-31733-0.
- J.W. Cooley, J.W. Tukey, "An algorithm for the Machine Calculation of Complex Fourier Series", *Math. Comp.* Vol. 19 (90), pp. 297-301, 1965.
- R.B. Randall, "Frequency analysis", Naerum: Brüel & Kjaer, 1987, ISBN 87-87355-07-8.

# FROM SIGNAL ANALYSIS TO SYSTEM ANALYSIS

**AUTHORS' NOTE**

Pieter Nuij, senior system architect, and David Rijlaarsdam, group leader, both work at NTS Systems Development in Eindhoven, the Netherlands.

[pieter.nuij@nts-group.nl](mailto:pieter.nuij@nts-group.nl)  
[www.nts-group.nl](http://www.nts-group.nl)

Following the previous article on signal analysis, this article focuses on system analysis, specifically on the Frequency Response Function (FRF) as a tool to describe the frequency-dependent behaviour of linear time-invariant systems. This article will outline the move from signal analysis to system analysis and then explain the concept of the cross-spectrum, the FRF and the coherence function. Finally, it will address the specific problems that arise in the identification of closed-loop systems, paying special attention to the practical aspects of FRF measurements.

PIETER NUIJ AND DAVID RIJLAARDAM

## Input-output relationship

In the time domain, the input-output relationship of a causal, linear, time-invariant system is described using a differential equation (DE). Figure 1 shows a mass-spring-damper system with input force  $f(t)$  and output displacement  $x(t)$ .

The DE describes the input-output relationship:

$$f(t) = m\ddot{x}(t) + d\dot{x}(t) + cx(t)$$

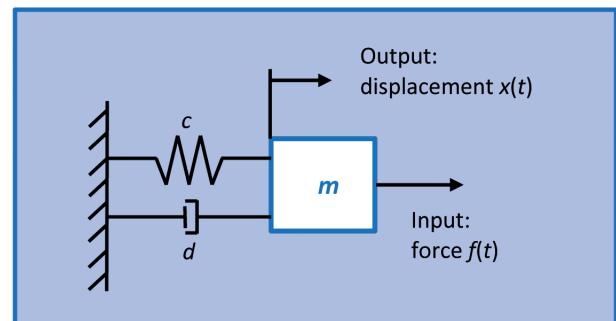
with  $m$  representing the mass,  $d$  the damping coefficient and  $c$  the stiffness. Although this equation describes the dynamics of the system completely, it requires solving for  $x(t)$  to explicitly relate the displacement to the excitation force. For more complex systems, solving the DE is often a tedious job. An alternative to solving the DE in the time domain is to transform the DE to the Laplace domain using the Laplace transform. The Laplace transform  $L\{f(t)\}$  is defined as:

$$F(s) = \int_0^\infty e^{-st} f(t) dt$$

with complex parameter  $s = \sigma + j\omega$ . As a result of this transformation,  $f'(t) = \frac{d}{dt}f(t)$  in the time domain becomes a multiplication with ' $s$ ' in the Laplace domain:

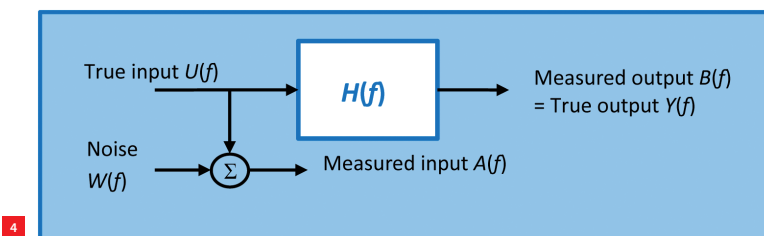
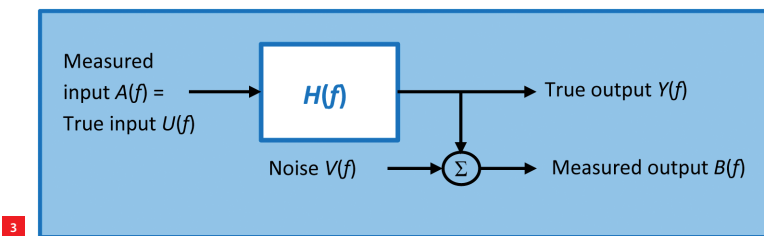
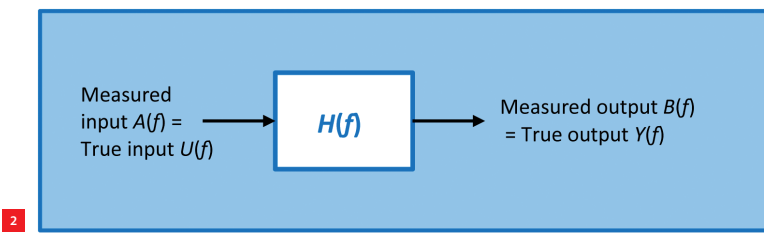
$$L\{f'(t)\} = sF(s) - f(0)$$

- 1 Mass-spring-damper system loaded with excitation force  $f(t)$  responds with displacement  $x(t)$ .



## Three articles

In a series of three articles on Frequency Response Function (FRF) measurements, this second article introduces the FRF, explaining the choice of test signals in relation to the coherence function and the measurement of the FRF in open- and closed-loop systems. The first article, which was published in the previous issue of Mikroniek, covered the steps necessary to convert a time-continuous signal into a discrete spectrum. Potential errors caused by aliasing and leakage were explained and solutions were presented. An overview of several types of test signals was presented. The third article will focus on the extension of frequency-domain methods towards nonlinear systems and the application of such methods to define and optimise the performance of such systems. Each article is illustrated with examples.



Applying this transformation to the DE results in:

$$F(s) = ms^2 X(s) + dsX(s) + cX(s)$$

assuming  $f'(0) = f(0) = 0$

From this expression, the input-output relationship becomes a polynomial expression with variable  $s$ :

$$\frac{X(s)}{F(s)} = \frac{1}{ms^2 + ds + c}$$

which is called the transfer function. Next, substituting  $s = j\omega = j2\pi f$  in the transfer function results in the FRF:

$$\frac{X(f)}{F(f)} = \frac{1}{(j2\pi f)^2 m + j2\pi f d + c}$$

$X(f)$  and  $F(f)$  are the Fourier transforms of  $x(t)$  and  $f(t)$ , so the FRF of a dynamic system can be determined from its input excitation signal and the resulting output response time signal using a fast Fourier transform (FFT) analyser. This is correct from a theoretical point of view, but the estimate will be biased if the influence of measurement noise is not taken into account, as will be discussed in the next section.

### Bias errors in FRF estimates

As discussed in the previous section, the FRF can be calculated from the Fourier transforms of the input and output signals of the system to be described. In the ideal situation as shown in Figure 2, the FRF calculation will yield an unbiased estimate:

$$\frac{B(f)}{A(f)} = \frac{Y(f)}{U(f)} = H(f)$$

It is clear that the signal  $U(f)$  must contain power in the frequency lines of interest to generate proper results. Without a proper excitation, no estimate is possible. In practice, the measured signals will always include a certain amount of noise. In the situation with noise  $V(f)$  in the output signal, as shown in Figure 3, the FRF estimate will be biased:

$$\frac{B(f)}{A(f)} = H(f) + \frac{V(f)}{A(f)}$$

Moreover, noise in the input signal, as shown in Figure 4, will also result in a biased FRF estimate:

$$\frac{B(f)}{A(f)} = H(f) \left[ 1 - \frac{W(f)}{A(f)} \right]$$

Since noise is always present in realistic measurements, the calculation of the FRF from the Fourier-transformed time signal  $A(t)$  and  $B(t)$  will always be biased. A significant improvement in the estimation of the FRF can be achieved by using the cross-spectrum. This will be introduced in the next section.

### The auto-spectrum and the cross-spectrum

The Fourier transform of a time signal  $a(t)$  is defined as:

$$A(f) = F\{a(t)\} = \int_{-\infty}^{+\infty} a(t) e^{-j2\pi ft} dt$$

## Certified Precision Engineer competencies

The content of this series of three articles is in part covered in the "Experimental Techniques in Mechatronics" course, provided by The High Tech Institute (HTI). This course has been selected for the DSPE Certification Program (see page 26).



and results in a complex spectrum  $A(f)$  with magnitude and phase information describing the cosine components that approximate the time signal  $a(t)$ . The auto-spectrum of  $a(t)$  is defined as:

$$S_{AA}(f) = A^*(f) \cdot A(f)$$

where  $*$  indicates the complex conjugate. Since the FFT routine only uses a finite-length time record of length  $T$  of the signal  $a(t)$ , the result is an estimate  $\hat{A}_i(f)$  of the true Fourier transform  $A(f)$  at the frequencies  $k \cdot \Delta f = k/T$ . From these individual estimates, the true auto-spectrum of  $a(t)$  can be calculated by averaging over  $n$  measurement records:

$$S_{AA}(f) = \lim_{n \rightarrow \infty} \frac{1}{n} \sum_{i=1}^n \hat{A}_i^*(f) \cdot \hat{A}_i(f)$$

Unlike the complex spectrum  $A(f)$ , the auto-spectrum  $S_{AA}(f)$  is real and describes the power distribution as a function of frequency.

The cross-spectrum  $S_{AB}(f)$  between the time signals  $a(t)$  and  $b(t)$  is defined by:

$$S_{AB}(f) = A^*(f) \cdot B(f)$$

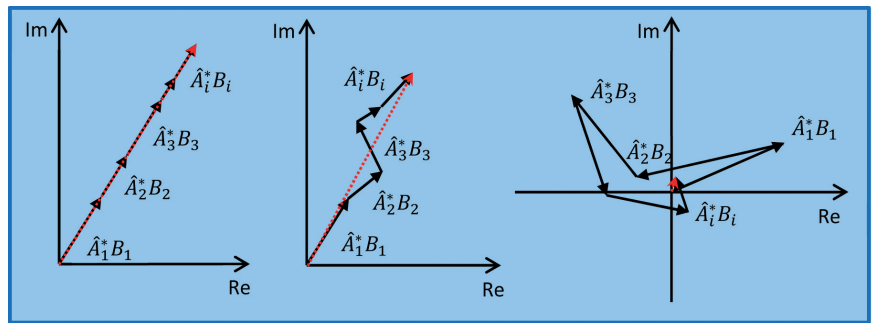
and can be calculated using the FFT by averaging the individual cross-spectra estimates:

$$S_{AB}(f) = \lim_{n \rightarrow \infty} \frac{1}{n} \sum_{i=1}^n \hat{A}_i^*(f) \cdot \hat{B}_i(f)$$

Unlike the auto-spectrum  $S_{AA}(f)$ , the cross-spectrum  $S_{AB}(f)$  is complex valued. The magnitude of each individual cross-spectrum estimate is the product of the magnitudes of the two individual signal components with frequency  $f_k$ . The phase of the cross-spectrum is the phase difference  $\Delta\phi(f_k)$  between the corresponding frequency components  $\hat{A}(f_k)$  and  $\hat{B}(f_k)$ .

Since the averaging operation is done on complex values, the magnitude of the averaged cross-spectrum will also depend on the variation of  $\Delta\phi(f_k)$  over the measurement records as can be seen in Figure 5. If two signals are uncorrelated, the phase difference  $\Delta\phi(f_k)$  will be random and the magnitude of the averaged cross-spectrum will be zero (see Figure 5c).

The cross-spectrum emphasises common frequency components in both signals, with a consistent phase relationship. This characteristic will be used in all practical measurements where noise is always present. In the second part of this paper, the variables in all derivations are assumed to be a function of frequency and the notation ' $(f)$ ' is left out in the formulae for clarity.



5a

5b

5c

**5** Averaging of cross-spectrum estimates for increasing variation in  $\Delta\phi(f_k)$ .

- (a) No phase variation and fully correlated.
- (b) Some phase variation but still correlated.
- (c) Fully uncorrelated.

### The $H_1$ and $H_2$ frequency response function estimators

The previous section explained that the averaged cross-spectrum of two uncorrelated signals is zero. This property will be used to determine a better estimate of the FRF in the case of noise in the input and output measurements as depicted in Figures 3 and 4. For noise in the output measurement (see Figure 3), the following relationships hold:

$$\begin{aligned} B &= H \cdot A + V \\ A^* \cdot B &= H \cdot A^* \cdot A + A^* \cdot V \\ \frac{A^* \cdot B}{A^* \cdot A} &= H + \frac{A^* \cdot V}{A^* \cdot A} \\ H_1(f) &= \frac{S_{AB}(f)}{S_{AA}(f)} \quad \text{if } S_{AV}(f) = 0 \end{aligned}$$

*[v(t), a(t) uncorrelated]*

Likewise for the situation of noise in the input measurement, as shown in Figure 4, the unbiased estimate for the FRF can be calculated using:

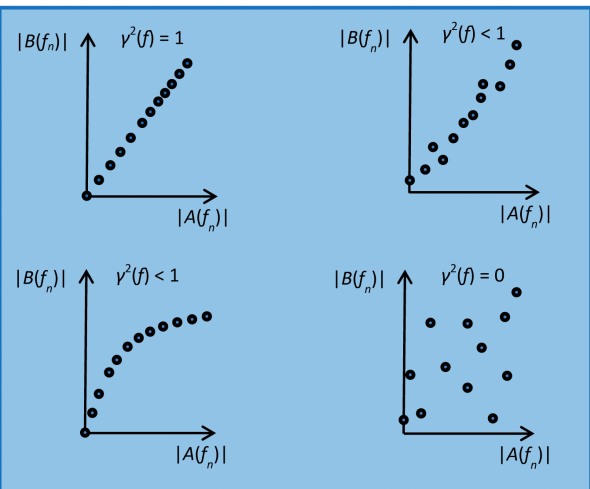
$$\begin{aligned} H_2(f) &= \frac{S_{BB}(f)}{S_{BA}(f)} \quad \text{if } S_{BV}(f) = 0 \\ &\quad [w(t), b(t) \text{ uncorrelated}] \end{aligned}$$

In both cases, the excitation signal is expected to be uncorrelated with the noise components in the measured input and output signals. This is always the case if the excitation signal is a random signal.

### The coherence function

In system analysis, it is important to quantify the degree of linear relationship between the input and output signals. In statistics, this relationship is indicated by the correlation coefficient, while in the frequency domain, it is indicated by the coherence function  $\gamma^2(f)$ :

$$\gamma^2(f) = \frac{|S_{AB}(f)|^2}{S_{AA}(f) \cdot S_{BB}(f)} \quad 0 \leq \gamma^2(f) \leq 1$$



6

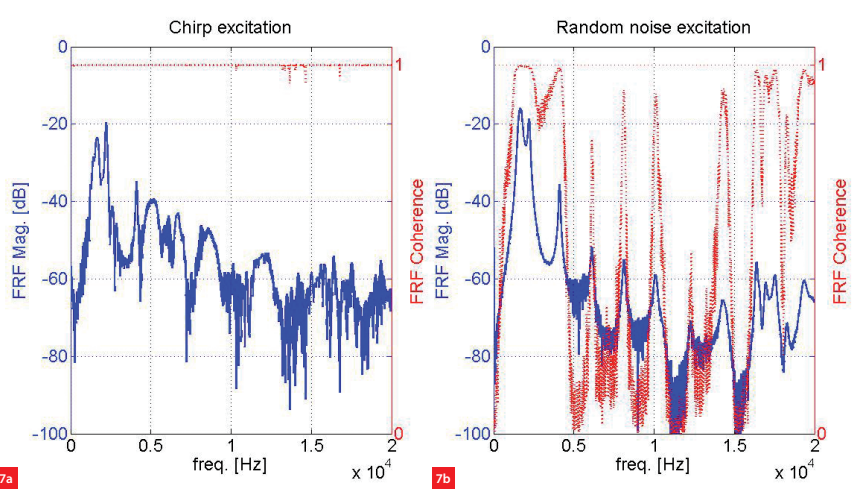
Figure 6 shows the relationship between the frequency components at frequency  $f_n$  of signal  $A(f)$ , which is the measured input of a system, and  $B(f)$ , which is measured at the output. Figure 6a clearly shows that the input-output relationship is linear and the coherence is equal to one. The input-output relationship in Figure 6b is no longer a straight line through the origin, but varies due to noise in either or both the measurement signals. Consequently, the coherence is less than one. Figure 6c shows a perfect, noise-free, non-linear relationship between the input and output signals and again the coherence is less than one. Figure 6d shows the situation where input and output signals are not related, resulting in a coherence equal to zero.

A coherence value less than one can be caused by:

- Nonlinear system behaviour.
- Noise in the measurements of  $a(t)$  and/or  $b(t)$ .
- Leakage in the FFT.
- Time-variant system behaviour.

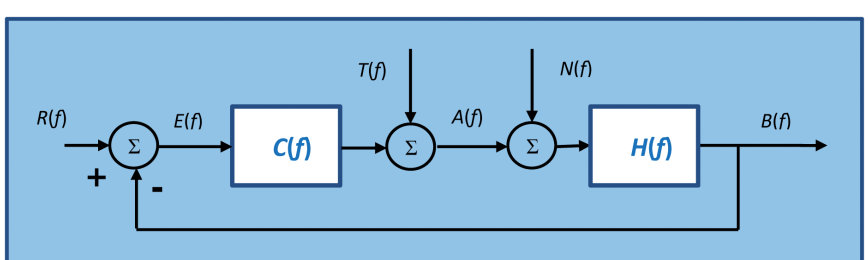
It is a common misunderstanding that a measurement with a coherence equal to one is proof of linear system behaviour. If the measurement is based on only one data block, i.e. without averaging across additional data blocks, coherence will always be equal to one even in the case of nonlinear system behaviour. Even if the coherence is determined using averaging, all deterministic test signals will yield a coherence value close to one if there is minimal measurement noise compared to the test signal. Examples of these types of test signals are the multi-sine and the hammer impact if all impacts are equally strong.

Figure 7a shows the FRF and coherence of a measurement of a nonlinear system using chirp excitation. The coherence is clearly one over most of the frequency range, which



7a

7b



8

contradicts the fact that the system is known to be nonlinear. Figure 7b shows the results for the same system, this time, however, measured with a random noise signal with the same RMS value used in the chirp excitation. The random noise excitation yields a coherence which is clearly less than one over most of the frequency range, as is to be expected for a nonlinear system.

### FRF estimation in closed-loop systems

Unlike open-loop systems, closed-loop systems include a feedback path between output and input. This feedback can cause unexpected problems in the FRF identification. Figure 8 is a model of a closed-loop system with controller  $C(f)$  and plant  $H(f)$  with setpoint  $R(f)$ , test signal  $T(f)$  and external noise  $N(f)$  acting on the system.

Any attempt to determine  $H(f)$  directly from the measured input signal  $A(f)$  and the measured output signal  $B(f)$  will fail because of the correlation between  $N(f)$  and  $A(f)$  and  $R(f)$  and  $A(f)$ :

$$\begin{aligned} B &= H(N + T + CR - CB) \rightarrow & B(1 + CH) &= H(N + T + CR) \\ A &= T + C(R - H(N + A)) \rightarrow & A(1 + CH) &= T + C(R - HN) \\ \frac{B}{A} &= H \frac{N + T + CR}{T + C(R - HN)} \rightarrow & \frac{S_{AB}}{S_{AA}} &= H \cdot \frac{S_{AN} + S_{AT} + CS_{AR}}{S_{AT} + C(S_{AR} - HS_{AN})} \end{aligned}$$

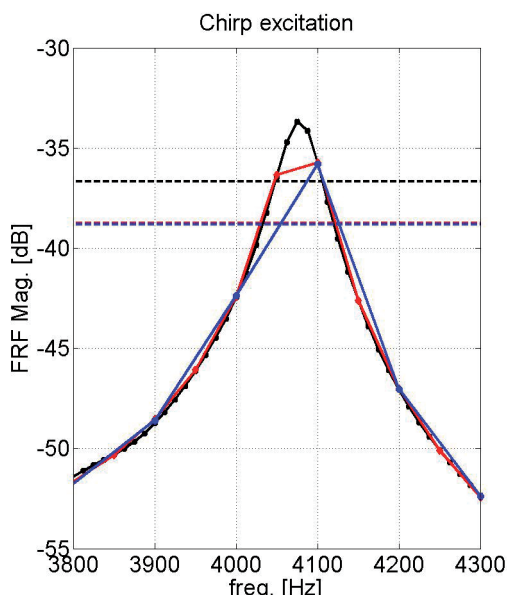
**6** The coherence function quantifies the amount of linearity between input signal component  $A(f_n)$  and output signal component  $B(f_n)$ .

**7** FRF (in blue) and coherence (in red) of a nonlinear system.

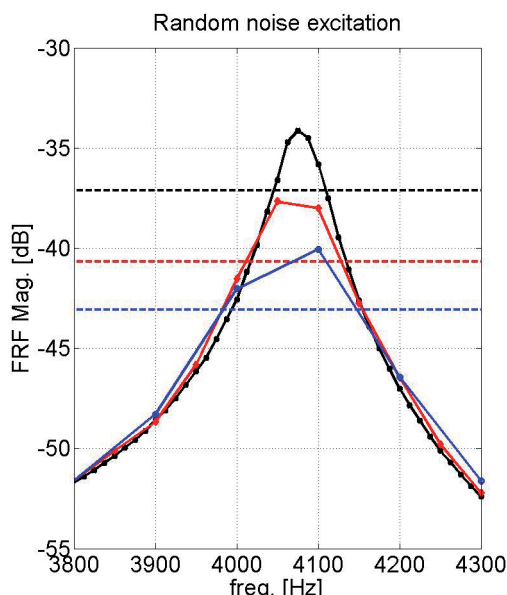
(a) Determined with a chirp, a deterministic signal.

(b) Measured with a random noise excitation.

**8** Closed-loop system with  $R(f)$  setpoint,  $T(f)$  test signal and  $N(f)$  external noise source acting on the system.  $A(f)$  is the measured input signal,  $B(f)$  is the measured output signal.



9a



9b

**9** FRF of a resonance. The horizontal lines indicate the -3dB magnitude levels of the respective resonances.  
 (a) Measured with a chirp.  
 (b) Measured with white noise.

Even if the setpoint signal  $R(f)$  is equal to zero, the estimate of  $H(f)$  will remain biased:

$$\frac{S_{AB}(f)}{S_{AA}(f)} = H(f) \cdot \frac{S_{AN}(f) + S_{AT}(f)}{S_{AT}(f) - C(f)H(f)S_{AN}(f)}$$

Depending on the signal-to-noise ratios in the loop, the estimate of the FRF of the plant may vary between  $H(f)$  and  $-1/C(f)$ .

A robust alternative to determine the plant FRF  $H(f)$  in a closed-loop system is the three-point method in which the sensitivity  $S(f)$  and the process sensitivity  $PS(f)$  are determined:

$$S(f) = \frac{S_{TA}}{S_{TT}} = \frac{1}{1+CH} + \frac{C}{1+CH} \left( \frac{S_{TR} - HS_{TN}}{S_{TT}} \right) = \frac{1}{1+C(f)H(f)}$$

$$PS(f) = -\frac{S_{TE}}{S_{TT}} = \frac{H}{1+CH} - \frac{1}{1+CH} \left( \frac{S_{TR} - HS_{TN}}{S_{TT}} \right) = \frac{H(f)}{1+C(f)H(f)}$$

$$H(f) = \frac{PS(f)}{S(f)}$$

if  $R(f)$ ,  $T(f)$  and  $N(f)$  are uncorrelated, and averaged spectra and cross-spectra are used.

### Tips for measuring an FRF in practice

Although a thorough understanding of the theory behind the FRF helps, it does not guarantee good measurement results. Experience with experimentation is also required for good results. This section focuses on some practical measurement aspects.

#### Choose the proper input and output signals

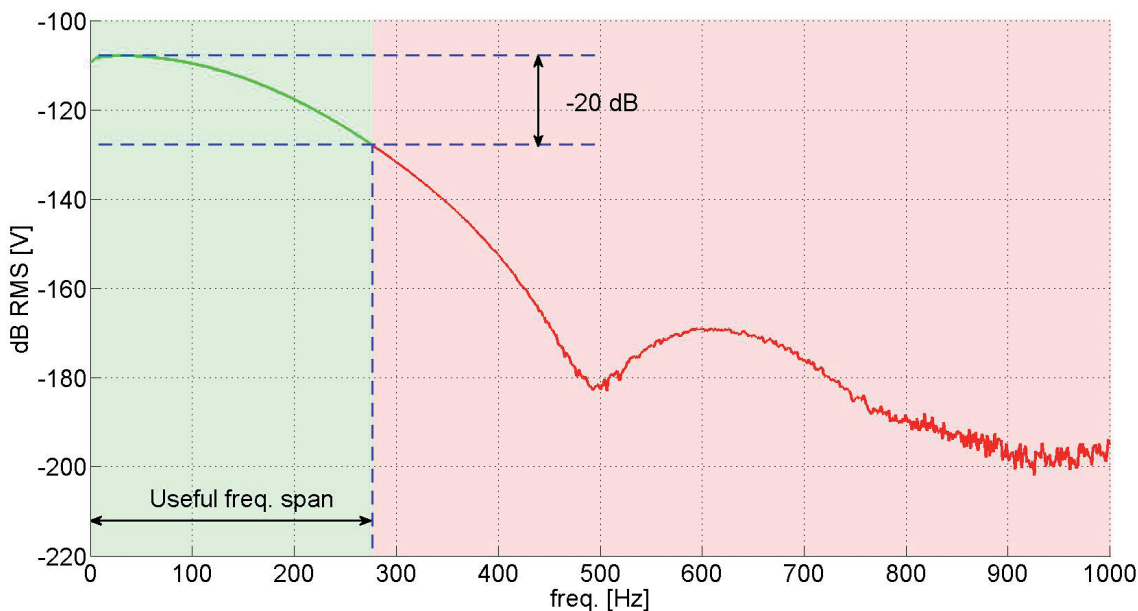
The choice of input and output signal is often determined by the accessibility of the signals. Measuring torque is often

difficult, but the torque signal can be calculated from a simple motor current measurement if the motor constant is known. Measuring small displacements at high frequencies with a good signal-to-noise ratio is often difficult, while measuring accelerations at high frequencies is simple because of the increase in sensitivity with  $(j2\pi f)^2$ . The corresponding FRF can be calculated by dividing the FRF by  $(j2\pi f)^2$ . Time spent on optimising the signal-to-noise ratio of the measurement signals is time well spent.

#### Choice of frequency range and frequency resolution

Take a broad frequency range for the first measurement to get a good general overview of the region of interest. In the subsequent measurements, however, limit the frequency range to the region of interest so as not to excite system dynamics outside that range. The required frequency resolution of the measurement depends on the damping at the resonances or antiresonances. Too coarse a resolution will underestimate the magnitude at the resonance frequency because of the ‘picket fence effect’. A very narrow resolution will not result in any additional quality improvement; it will only result in unnecessary measurement time.

Figure 9a shows the measurements of a resonance at three different frequency resolutions with a chirp test signal under leakage-free conditions. The estimate of the resonance magnitude depends on the frequency resolution used and shows a 2.2dB variation. As a rule, a resonance is estimated correctly if the frequency interval between the -3dB magnitude frequencies is covered by at least five frequency lines. Figure 9b shows the measurement results of the same system but with a random noise test signal.



10

Apart from the ‘picket fence effect’, leakage errors are also evident. These errors show up as a difference in the magnitude values for the same frequency line as a function of the resolution. Even using a Hanning weighting function, these differences amount to approximately 4 dB at 4,100 Hz.

#### *Hammer or shaker excitation for modal analysis?*

The choice of excitation is often dictated by practical considerations like the accessibility of the test object, the ease of mounting a shaker and the required frequency range of excitation. In the case of impact excitation, the tip of the hammer determines the width of the excitation spectrum. The useful frequency range starts at 0 Hz and is limited to that frequency at which the magnitude is 20 dB less than the low-frequency magnitude, as can be seen in Figure 10.

When testing very sensitive equipment, shaker excitation is often preferred over impact excitation. A band-limited white noise test signal in combination with a Hanning weighting function is a good starting point because the total signal power is evenly distributed over the frequency range of interest. This reduces the risk of over-driving resonances, which can happen with a sinusoidal excitation signal. Moreover, because random noise is not a deterministic signal, the information from the coherence function can be used to assess the linearity of the measurement.

#### *Optimise the signal-to-noise ratio of the signals*

A dip in the coherence function often coincides with a low value in the excitation and/or response spectra. If the magnitude at the anti-resonance frequency is relevant, increasing the signal-to-noise ratio by increasing the input

**10** *The –20dB rule to determine the useful frequency range in the case of impact excitation.*

power in this frequency range is an option. Other options are zoom measurements in that limited frequency range. This will allow the signal conditioning to be optimised to reduce the quantisation noise.

#### *Reduce unnecessary nonlinear behaviour as much as possible*

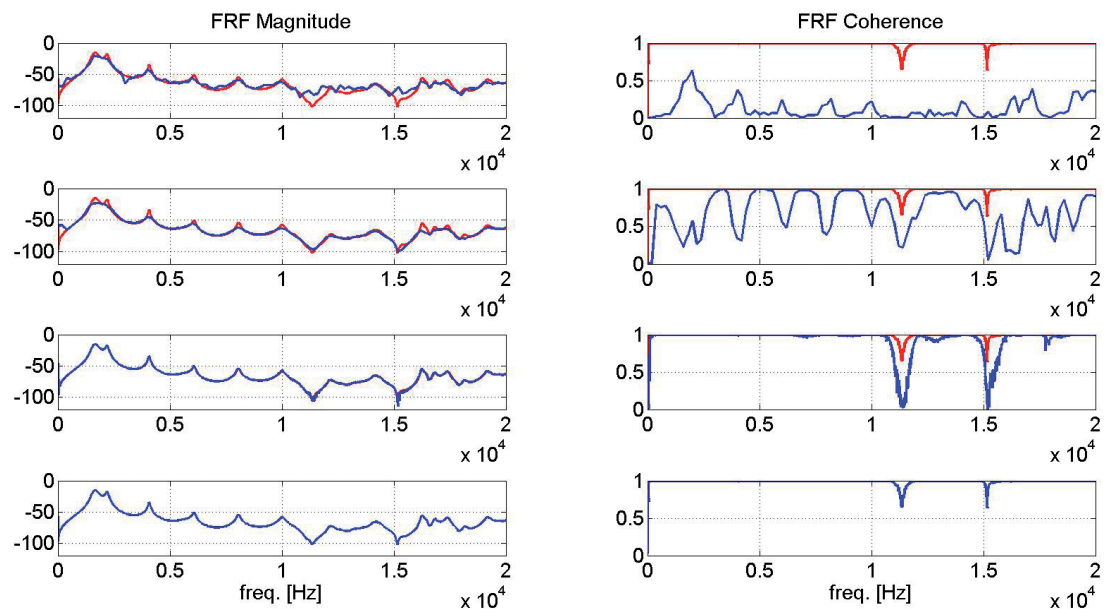
All real systems are in essence nonlinear, but for many systems, under normal operating conditions, the nonlinear behaviour can be ignored if the measurements are carried out carefully. Do not over-drive the system, check for saturating power amplifiers and overloaded sensors. Listen for rattles in coverings, check for strong 50/60Hz harmonics. Optimise the sensor signal-to-noise ratio and choose proper ADC input ranging. Prevent aliasing and reduce leakage.

#### *Do the FRF measurements under the proper operating conditions*

Friction in positioning systems often induces stick-slip behaviour. The stick phase system dynamics are very different from the dynamics in the slip phase. For FRF measurements in the stick phase, only very small excitations are allowed in the 100 nm range. The slip phase dynamics can be measured reliably by jogging the system.

#### *Be critical about the measurement results*

Figure 11 shows a typical evolution in the quality of an FRF measurement. The excitation signal is band-limited white noise. The left column shows the magnitudes of the FRF measurements, while the right column shows the corresponding coherence plots. In both columns, the red curves represent the final results. In the upper row in blue, a



11

frequency resolution of 200 Hz was used with a rectangular weighting function. Both large leakage errors and picket fence errors are present.

The second row shows the results for a measurement with equal excitation signal level and frequency resolution but with a Hanning weighting function. The increase in coherence is caused by a significant reduction in leakage error. The picket fence error is not reduced. The coherence function still shows ranges with low values, however. These ranges coincide with the resonances and antiresonances. There are different reasons for the low coherence values of the resonances and antiresonances. In the case of the resonances the low coherence is due to leakage, while in the case of the antiresonances the low coherence is caused by low signal-to-noise ratios, as will become evident from the subsequent measurements.

With the same excitation signal level and weighting function as in row two, the measurement in the third row is done with a frequency resolution of 6.25 Hz. Once again, the leakage error is reduced as indicated by the increased value of the coherence function. The picket fence error is also reduced. The remaining minima in the coherence function coincide with the antiresonances. The bottom row shows the final results. In this measurement, the RMS value of the excitation signal is increased by a factor of 10, which results in an increased signal-to-noise ratio of the output signal. This results in a better coherence for the antiresonances. One should be careful about increasing the excitation signal any further, as this may over-drive the system resulting in a lower coherence value due to the induced nonlinearity. ■

**11** FRF estimates for various weighting functions, frequency resolutions and excitation levels.

### Coming up in Part 3

Part 3 will introduce frequency domain methods to use in practice to model and optimise the performance of nonlinear systems. The article provides a brief overview and experimental examples of existing modelling techniques and a novel method to assess and optimise the performance of nonlinear systems using frequency domain-based tooling.

#### LITERATURE

- P. Nuij, D. Rijlaarsdam, "Introduction to Frequency Response Function Measurements (Part 1)", *Mikroniek*, Vol. 54 (2), pp. 8-13, 2014.
- J.S. Bendat, A.G. Piersol, *Engineering applications of Correlation and Spectral Analysis*, Chichester: Wiley-Interscience, 1993, ISBN: 0-471-57055-9.
- H. Herlufsen, "Dual Channel FFT Analysis (Part 1)", *Brüel & Kjær Technical Review*, No. 1, 1984.

# FREQUENCY DOMAIN MODELLING AND PERFORMANCE OPTIMISATION OF NONLINEAR SYSTEMS

## AUTHORS' NOTE

David Rijlaarsdam, group leader, and Pieter Nuij, senior system architect, both work at NTS Systems Development in Eindhoven, the Netherlands. Maarten Steinbuch is full professor in the department of Control Systems Technology at Eindhoven University of Technology. Johan Schoukens is full professor in the department of Fundamental Electricity and Instrumentation at the Free University of Brussels (VUB), Belgium.

david.rijlaarsdam@nts-group.nl  
www.nts-group.nl

Concluding a series of three, this article deals with frequency domain methods when applied to systems subject to nonlinear dynamical effects. To meet increasing system requirements, techniques have to deal with the performance-degrading effects of nonlinearities. When applied with care, frequency domain methods provide practically applicable tools to model and optimise the performance of nonlinear systems. This article provides a brief overview and experimental examples of existing modelling techniques, as well as a novel method for performance assessment and optimisation using frequency domain based tooling.

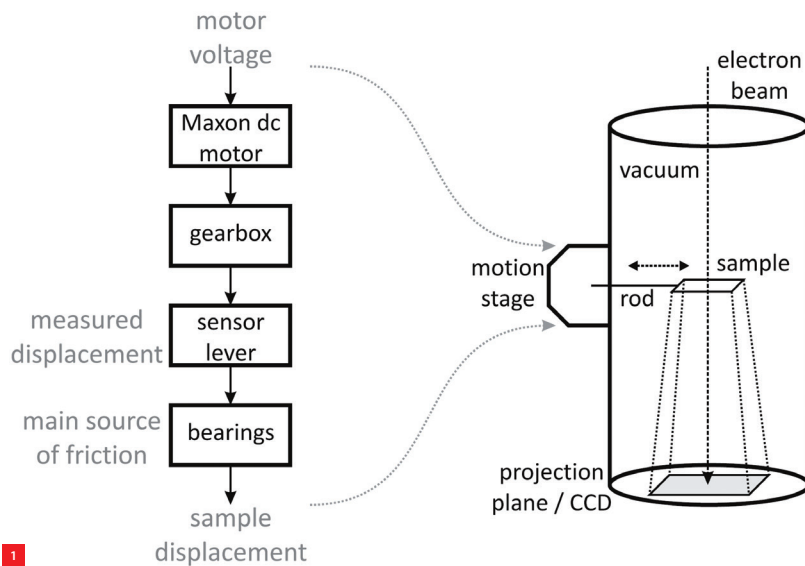
DAVID RIJLAARDAM, PIETER NUIJ, MAARTEN STEINBUCH AND JOHAN SCHOUKENS

## Three articles

In a series of three articles on Frequency Response Function (FRF) measurements, this third article focusses on the extension of frequency-domain methods towards nonlinear systems and the application of such methods to define and optimise the performance of such systems. The first article [1] covered the steps necessary to convert a time-continuous signal into a discrete spectrum. Potential errors caused by aliasing and leakage were explained and solutions were presented. An overview of several types of test signals was presented. The second article [2] introduced the FRF, explaining the choice of test signals in relation to the coherence function and the measurement of the FRF in open- and closed-loop systems. Each article is illustrated with examples.

## Introduction

Increasing performance requirements on high-performance (motion) systems require novel techniques to deal with performance-degrading effects of nonlinearities. For linear and time-invariant (LTI) systems, frequency domain methods are widely accepted in the engineering community for modelling as well as performance optimisation purposes. Although systems may be specifically designed to minimise nonlinear effects, nonlinearities such as magnetic fields may be inherently present in the design. In particular, some applications require the presence of nonlinear effects, such as friction in the motion stage of an electron microscope. Whether performance is measured by speed, accuracy, reproducibility, smoothness, or other performance measures, the effects of nonlinearities become increasingly important in high-precision applications.



To accurately detect, analyse and compensate performance-degrading effects in controlled nonlinear dynamical systems, practically applicable tools are required. Therefore, following up on [1] and [2], this article discusses the pitfalls and potential gains when using frequency domain techniques to model and optimise the performance of nonlinear systems. Note that this article aims to provide an accessible, but very brief overview of existing methods to address nonlinear systems in the frequency domain. For a more complete and formal overview and comparison, see, for example, [3].

The main carrier throughout this paper is an industrial case study of optimal friction compensation in a Transmission Electron Microscope (TEM) system as depicted in Figure 1.

## Certified Precision Engineer competencies

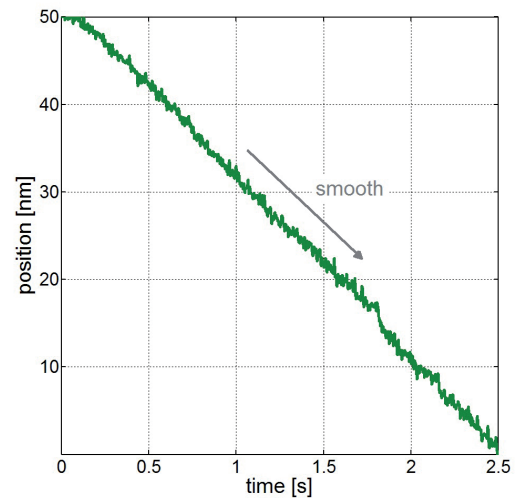
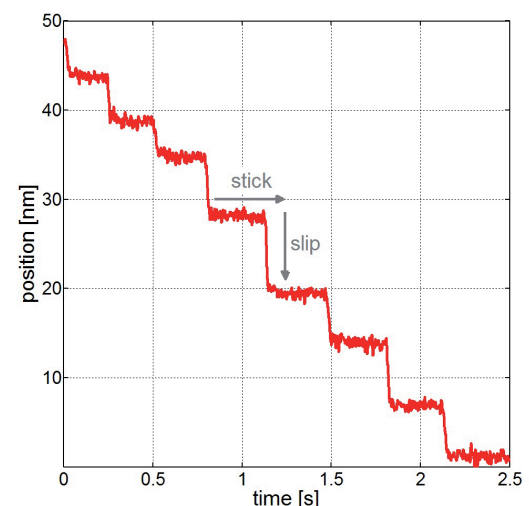
The content of this series of three articles is in part covered in the "Experimental Techniques in Mechatronics" course from Mechatronics Academy, offered to the market by The High Tech Institute. This course has been selected for the DSPE Certification Program (see page 46).

[WWW.DSPEREGISTRATION.NL](http://WWW.DSPEREGISTRATION.NL) | [WWW.HIGHTECHINSTITUTE.NL](http://WWW.HIGHTECHINSTITUTE.NL)  
[WWW.MECHATRONICS-ACADEMY.NL](http://WWW.MECHATRONICS-ACADEMY.NL)



1 Schematic depiction of the (motion module) of the TEM system. For simplicity, only one direction of motion is depicted. All transfer functions in this article are computed from the motor voltage to the measured displacement.

2 Low-speed jogging response of the TEM system and the effect of optimised friction compensation.  
 (a) No Coulomb friction feed forward.  
 (b) Optimal Coulomb friction feed forward.

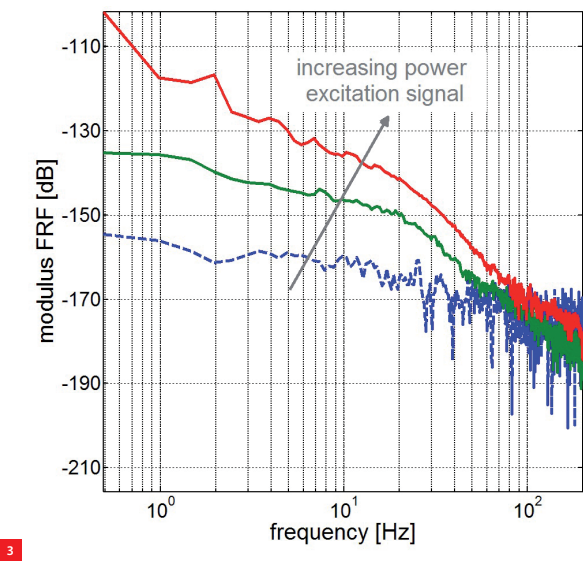


Based on this example the effects of nonlinearities in the frequency domain are introduced as well as state-of-the-art modelling techniques. Moreover, a practically applicable method is introduced to analyse, visualise and optimally compensate performance-degrading nonlinear effects in dynamical systems. Application of this technique has resulted in a reduction of the achievable smooth jogging motion to a level of 20 nm/s in an industrial TEM (Figure 2) [4].

## Frequency domain modelling of nonlinear systems

### Overview of modelling techniques

Frequency domain methods are widely accepted and have been an impetus for the development of modelling and



**3** Frequency response function of the TEM for varying input levels.

control design techniques for LTI systems. Although the linearity assumption can rarely be satisfied in practice, linear models and analysis often suffice when systems are operated around a given working point. Given the widespread acceptance and success of frequency domain methods for LTI systems, several approaches exist that extend frequency domain methods towards nonlinear systems, e.g. the Generalised Frequency Response Function (GFRF) [5], nonlinear FRF [6], describing functions [7] and linear approximations [8]. Table 1 provides an overview of such methods and the nonlinear effects / information captured by each model.

The success and popularity of frequency domain methods for LTI systems is largely due to the combination of Fourier analysis and the fact that a sine wave is an eigenfunction of LTI systems, which satisfy the properties of superposition and homogeneity. For nonlinear systems, this is generally not the case, which implies that a conventional frequency domain model captures only a part of the system's dynamics, as illustrated by Figure 3.

Figure 3 depicts three Frequency Response Functions (FRFs) of the TEM system depicted in Figure 1. These FRFs are measured using white-noise inputs with three different rms values. It becomes clear that the FRF captures only a subset of the system's dynamics as the dependence of the dynamics on the input amplitude is not captured by a single FRF. This effect, called 'gain compression / expansion', is one of several effects of nonlinear behavior in the frequency domain, such as desensitisation, intermodulation and the generation of harmonics (see Table 1). Moreover, although the coherence of a single FRF (not shown) may indicate nonlinear behavior if the excitation signal is random, it provides no indication of nonlinearity if the system is subject to a deterministic excitation signal such as a multi-/swept sine [8].

Hence, traditional frequency domain tools and models fail in the presence of nonlinearities, requiring an extension of conventional frequency domain methodologies if nonlinearities are present. Two modelling approaches will be discussed that allow detection and modelling of a subset of nonlinear effects in the frequency domain. Moreover, it

**Table 1** Overview of frequency domain modelling approaches for nonlinear systems.

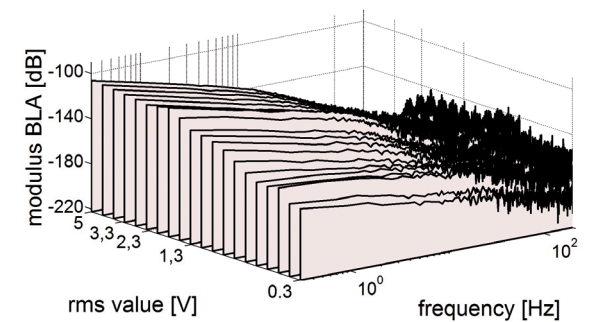
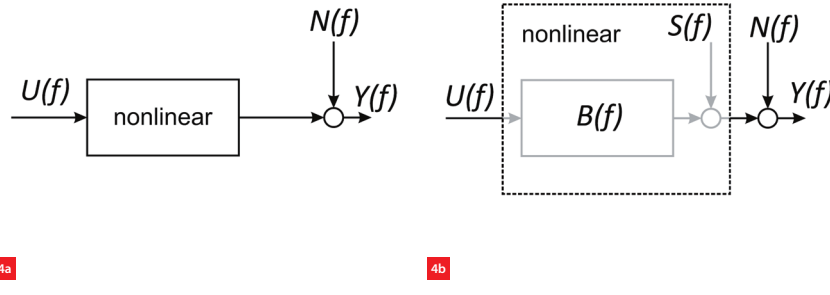
**Legend:**

**green:**  
effect captured / info available

**red:**  
effect not captured / info not available

**orange:**  
effect partly captured / info available,  
requires additional processing

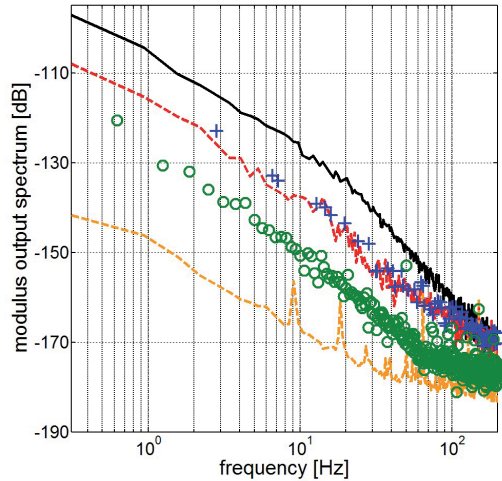
	Gain compression / expansion	Desensitisation	Intermodulation	Harmonics	Content at frequencies present in input	Content at frequencies not present in input
Conventional FRF						
Generalised FRF [5]						
Nonlinear FRF [6]						
Describing function	dependence of gain on input excitation level	dependence of response at one frequency on input at another frequency	combination of input frequencies to produce new frequencies in the output	generation of frequency components in output at multiples of input frequency	gain phase	gain phase
Best linear approximation [8]						



**4** Transformation of a nonlinear system to a best linear approximation (BLA) and corresponding nonlinear distortion.  
**(a)** Nonlinear system.  
**(b)** BLA and nonlinear distortion.

**5** Analysis of the TEM system.  
**(a)** Best linear approximation.  
**(b)** Output spectrum: average (black), variance due to nonlinearities (red) and stochastic disturbances (orange), also energy appearing at odd (blue) and even (green) non-excited frequencies.

5b



will be shown later on that analysis of nonlinear effects in the frequency domain provides a useful way to define and optimise the performance of nonlinear systems.

### Experimental results

In the following, two approaches to modelling the nonlinear TEM system are illustrated based on experimental results. The best linear approximation (BLA) and Higher Order Sinusoidal Input Describing Function (HOSIDF) are selected from Table 1 as they provide models that are easily computed from measured data and provide insightful representations, which are usable in practice. First, a best linear approximation of the TEM system is derived, yielding separate quality measures relating to random disturbances (noise) and nonlinear influences. Second, the HOSIDF is used to explicitly investigate nonlinear effects in the TEM system.

### Linearised modelling: best linear approximation

In this section, the estimation of a linear model in the presence of nonlinearities is addressed. Consider a nonlinear system as depicted in Figure 4a and assume the system can be transformed to a structure as in Figure 4b (for existence and invariance of this transformation, see [3]). In Figure 4b, the Fourier transform of the output  $Y(f)$  then depends on the input  $U(f)$  and consists of a component that is generated by an LTI system  $B(f)$ , a distortion  $S(f)$  due to nonlinearities and an output disturbance  $N(f)$ , i.e.

$$Y(f) = B(f)U(f) + S(f) + N(f)$$

Then, the pair  $(B(f), S(f))$  is defined as the best linear approximation (BLA) [8], if it satisfies:

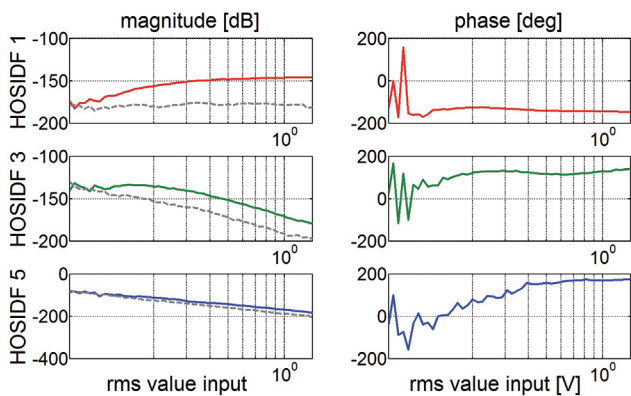
$$B(f) = \arg \min_{B(f)} E\{(y(t) - B(f)u(t))^2\}$$

Here,  $E\{\cdot\}$  denotes the expected value. Several studies concerning the existence and uniqueness of the BLA can be found [3] [8]. In this section, however, attention is focussed on practical identification of the BLA and the information available therein.

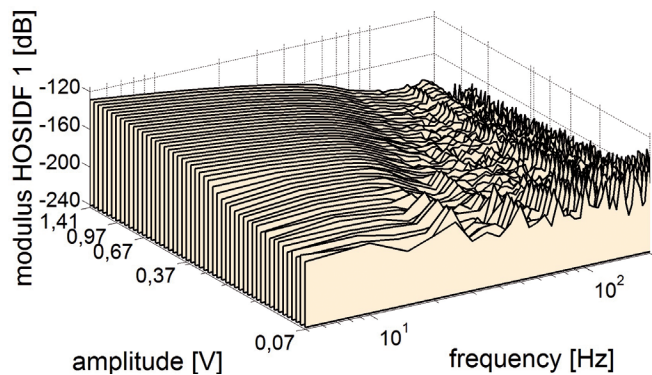
In this example, the BLA is derived by exciting the TEM system with a set of so-called ‘special random, odd multisines’, i.e. different realisations of multisine signals with equal amplitude spectra, but randomised phase realisations [8]. The adjectives ‘special’ and ‘odd’ refer to the fact that the multisine signal is constructed only from sinusoids which are an odd multiple of some base frequency and some of these odd multiples are set to zero in the excitation spectrum (‘special’). Such specially designed signals allow to:

1. compute the BLA on spectral lines which are present in the excitation signal;
2. detect nonlinearities by energy appearing at non-excited spectral lines (intermodulation, harmonics);
3. assess model quality by separately quantifying variance due to nonlinearities and output disturbances.

For details on the analysis required to attain the information mentioned above, see [3]. Figure 5a shows the BLA of the TEM system for different excitation levels (rms values of the multisine signal). Furthermore, Figure 5b shows the output spectrum generated by the BLA and the separation between the variance on this average due to nonlinear effects and due to output disturbances. Moreover,



6a



6b

it shows the energy level at non-excited odd and even multiples of the base frequency of the multisine which are not present in the excitation signal.

This shows that the variance caused by nonlinearities is mainly due to odd nonlinear effects, which points towards a point-symmetric nonlinearity such as (Coulomb) friction (a point-symmetric nonlinear function of the system's velocity). Hence, using the BLA when working with nonlinear systems not only provides a best approximation of the FRF, but yields both quantitative measures of the type and level of nonlinearities present and the quality of the measurement (signal-to-noise ratio).

#### Nonlinear modelling: Higher Order Sinusoidal Input Describing Functions

The second modelling approach specifically models the generation of harmonics due to nonlinearities. Due to its similarity to the classical sinusoidal describing function, the model is referred to as the Higher Order Sinusoidal Input Describing Function (HOSIDF) [7]. The HOSIDFs are defined for sinusoidal inputs with frequency  $f_0$ . The  $k^{\text{th}}$  HOSIDF  $H_k(f_0, a)$  is a function of both frequency  $f_0$  and amplitude  $a$  and is defined as follows:

$$H_k(f_0, a) = Y_s(kf_0, a) / U_s^k(f_0, a)$$

Here, the subscript  $s$  refers to the single-sided spectrum of the input  $U(f)$  and output  $Y(f)$ . For  $k = 1$ , the above definition equals the definition of a conventional FRF under sinusoidal excitation and that of a conventional sinusoidal describing function. The added value of the HOSIDFs comes from explicitly – both in gain and phase shift – modelling the generation of harmonic frequency components by the nonlinear system.

Figure 6a shows the first three odd HOSIDFs for the TEM system at  $f_0 = 20$  Hz for varying input amplitude.

- 6** Higher-order sinusoidal describing functions (HOSIDFs) of the TEM system.  
 (a) First, third and fifth HOSIDF for  $f_0 = 20$  Hz (grey: variance on average).  
 (b) First HOSIDF.

Furthermore, Figure 6b shows the first HOSIDF as a function of frequency and excitation amplitude. The fact that the even HOSIDFs are close to zero and the behaviour of the gain characteristics of the odd HOSIDFs, both point towards a point-symmetric nonlinearity, the effect of which reduces with increasing excitation amplitude, e.g. friction.

Apart from providing insight into and quantification of the nonlinear effects present, the HOSIDFs have been shown to allow computation of the parameters defining the nonlinearity. Moreover, the HOSIDFs can be used to optimally design nonlinear compensators to reduce performance-degrading effects in nonlinear systems. This is addressed in the next section.

#### Frequency domain performance optimisation of nonlinear systems

##### Time versus frequency domain performance

While the previous section dealt with modelling nonlinear effects in the frequency domain, this section focusses on using frequency domain analysis to optimise the performance of nonlinear systems [3] [4]. Defining and optimising performance of nonlinear systems in a practically applicable manner is nontrivial. For example, performance indicators for LTI systems such as bandwidth, sensitivity and gain/phase/modulus margin cannot be used and global optimisation of a given performance indicator is not straightforward.

The method introduced in the following is based on the concept behind the HOSIDFs, i.e. nonlinear effects generate harmonics when the system is subject to a sinusoidal input (often harmonics are indeed a necessary and sufficient condition for the existence of nonlinear behaviour [3]). The method also assumes that the nonlinear effects are performance-degrading and should therefore be

compensated. However, before moving to performance optimisation, consider the essential difference between time and frequency domain based performance assessment; see Table 2.

Table 2 illustrates the difference between optimisation based on time and frequency domain analysis with respect to performance in terms of tracking and compensation of nonlinear effects. If a control system is optimised based on tracking error, the output of such a system will approximate the sinusoidal reference in both amplitude and phase (light red). The controller will, however, sub-optimally compensate the nonlinearity as the input-dependent term in the performance measure clouds the influence of the harmonics generated by the nonlinearity (dark red). The resulting controller only provides optimal tracking for the amplitude and frequency of the signal applied during tuning.

If instead the harmonics are optimally compensated by minimising the corresponding frequency domain performance measure only (dark green), the corresponding output will match the input in frequency, but possibly differ in amplitude and phase (light green) resulting in a sub-optimal tracking error. The solution comes from separating the problem and using the appropriate performance measure for each job [4]. Hence, first optimise a nonlinear controller to optimally compensate nonlinear effects based on a frequency domain performance measure (e.g. dark green) and then optimise a conventional LTI controller to achieve tracking performance and disturbance attenuation, e.g. using loop shaping.

Next, an example of frequency domain based friction compensation in a TEM is presented to illustrate the above.

#### *Frequency domain based friction compensation*

As indicated in Table 2, nonlinear effects can be assessed in the frequency domain by considering harmonics present in the output when the system is subject to a sinusoidal input. For example, the ratio between the energy present at

harmonics and at the excitation frequency (Table 2, dark green) provides a suitable and practically measurable performance measure. Note that optimising nonlinear compensators by removing harmonics in the output of a system provides a globally optimised controller for a large class of systems, including magnetic fields, actuator/sensor nonlinearities and several forms of friction. Hence, a static nonlinear compensator optimised in this way, provides optimal compensation for any input/reference signal, although it was tuned using a sinusoidal input only [3].

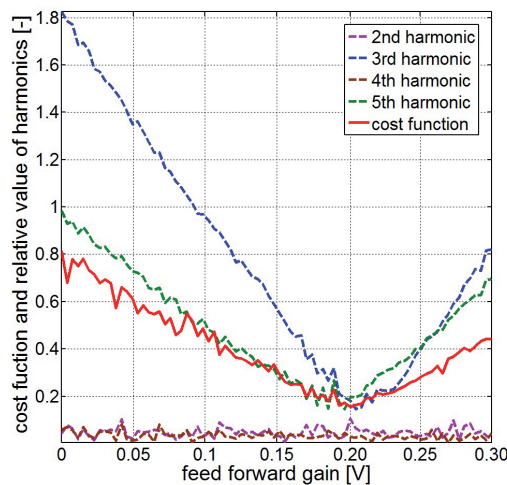
The method described above has, so far, been applied to optimise the performance of a military surveillance camera, linearise amplifier characteristics and compensate friction in a TEM motion module [4]. Moreover, simulations are successful in linearisation of the influences of magnetic fields in maglev applications and fully automated, adaptive implementations have been successfully applied in practice. For the purpose of this article, attention is focussed on the application of friction compensation in a TEM.

The TEM system depicted in Figure 1 is subject to conventional Coulomb friction feed forward and the corresponding feed-forward gain is to be optimally tuned. In this application the feed-forward gain is incrementally increased while the system is subject to a sinusoid with a frequency significantly below the bandwidth of the closed-loop system. The results are depicted in Figure 7.

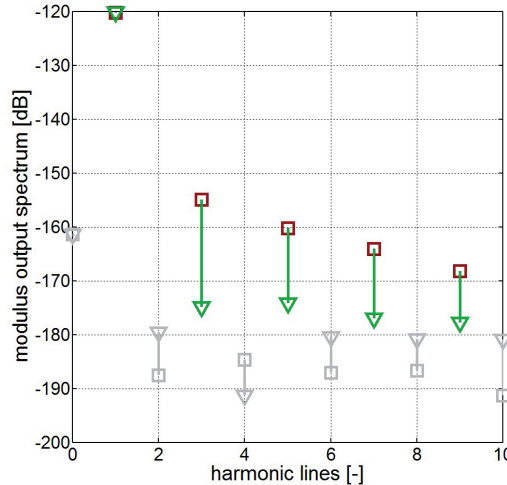
Figure 7a shows the energy present at the individual harmonic lines in the spectrum as a function of the feed-forward gain. Moreover, the cost function combining all statistically relevant harmonics is depicted. From Figure 7a it becomes clear that around 0.2 V the overall energy at harmonics in the output is minimised (individual harmonics have slightly different optima due to the nature of the nonlinearity and compensator). As observed in Figure 7b, the harmonics in the output spectrum have indeed been reduced significantly when comparing the uncompensated (red) and optimally compensated (green) situation.

**Table 2** Time and frequency domain performance measures for optimal tracking and nonlinear compensator design.

	Time domain	Frequency domain
Optimal nonlinear compensator	$A \cos(2\pi f_0 t + \varphi_0)$ $\downarrow$ $B \cos(2\pi f_0 t + \psi)$	minimise harmonic disturbance $\sum_{k=0}^K \frac{ Y(kf_0) }{ Y(f_0) }$ $k \neq 1$
Optimal tracking	$A \cos(2\pi f_0 t + \varphi_0)$ $\downarrow$ $A \cos(2\pi f_0 t + \varphi_0)$	minimise tracking error and harmonic disturbance $\sqrt{ Y(f_0) - U(f_0) ^2 + \sum_{k=0}^K  Y(kf_0) ^2}$



7a



7b

The practical implications and global nature of the optimised tuning become clear from Figure 2. Comparing Figure 2a and 2b yields that selecting the optimised parameter setting based on the frequency domain based performance measure depicted in Figure 7a yields a significant performance improvement in terms of smoothness during low-speed jogging motion at 20 nm/s.

### Conclusions

Although frequency domain methods are widely applied and accepted for modelling and performance optimisation of linear and time-invariant system, their applicability to systems containing nonlinearities is nontrivial. However, increasing performance requirements on high-performance systems require novel techniques to model and deal with the performance-degrading effects of nonlinearities. When applied with care, frequency domain methods provide practically applicable tools to model and optimise the performance of nonlinear systems. This article provides a brief overview of existing frequency domain based modelling techniques for nonlinear systems and a novel method to assess and optimise the performance of such systems. Both the modelling approach and performance optimisation are illustrated using a TEM (Transmission Electron Microscope) system suffering from the performance-degrading effects of friction during low-speed jogging motion.

### Acknowledgement

The work reported in this article was carried out as part of Condor, a project under the supervision of the Embedded Systems Institute (ESI) with FEI Company as the industrial partner. This project was partially supported by the Dutch

Ministry of Economic Affairs under the BSIK programme. This work was supported in part by the Fund for Scientific Research (FWO-Vlaanderen), by the Flemish Government (Methusalem), and by the Belgian Government through the Interuniversity Poles of Attraction (IAP VI/4) Programme. ■

**7** Frequency domain based optimisation of Coulomb friction feed forward in the TEM system.

(a) First five harmonics and performance measure (Table 2, dark green) as a function of controller parameter.

(b) Difference between the output spectrum without (red) and with (green) optimised Coulomb friction feed forward. Grey lines indicate statistically non-significant data.

### REFERENCES

- [1] P. Nuij and D. Rijlaarsdam, "Introduction to frequency response function measurements – Part 1", *Mikroniek*, 54(2):8-13, 2014.
- [2] P. Nuij and D. Rijlaarsdam, "Introduction to frequency response function measurements – Part 2", *Mikroniek*, 54(3):14-22, 2014.
- [3] D. Rijlaarsdam, *Frequency domain based performance optimization of systems with static nonlinearities*, Ph.D. thesis, Eindhoven University of Technology, ISBN: 978-90-386-3149-3, 2012 (available at [www.davidrijlaarsdam.nl](http://www.davidrijlaarsdam.nl)).
- [4] D. Rijlaarsdam, P. Nuij, J. Schoukens and M. Steinbuch, "Frequency domain based nonlinear feed forward control design for friction compensation", *Mechanical Systems and Signal Processing*, 27(2):551-562, 2012.
- [5] R. Yue, S. Billings and Z.-Q. Lang, "An investigation into the characteristics of nonlinear frequency response functions. Part 1: Understanding the higher dimensional frequency spaces", *International Journal of Control*, 78(13):1031-1044, 2005.
- [6] A. Pavlov, N. van de Wouw and H. Nijmeijer, "Frequency response functions for nonlinear convergent systems", *IEEE Transactions on Automatic Control*, 52(6):1159-1165, 2007.
- [7] P. Nuij, O. Bosgra and M. Steinbuch, "Higher-order sinusoidal input describing functions for the analysis of non-linear systems with harmonic responses", *Mechanical Systems and Signal Processing*, 20(8):1883-1904, 2006.
- [8] R. Pintelon and J. Schoukens, *System identification: a frequency domain approach*, Wiley-Blackwell, ISBN: 978-04-706-4037-1, 2012.